Smart Structures and Systems, Vol. 6, No. 7 (2010) 811-833
DOI: http://dx.doi.org/10.12989/sss.2010.6.7.811

Integrated vibration control and health monitoring of building structures: a time-domain approach

B. Chen*[1,2], Y.L. Xu[1] and X. Zhao[1]

[1]*Department of Civil and Structural Engineering, The Hong Kong Polytechnic University, Kowloon, Hong Kong, China*
[2]*Key Laboratory of Roadway Bridge and Structural Engineering, Wuhan University of Technology, Wuhan, China*

(Received August 12, 2008, Accepted November 17, 2009)

Abstract. Vibration control and health monitoring of building structures have been actively investigated in recent years but treated separately according to the primary objective pursued. This paper presents a general approach in the time domain for integrating vibration control and health monitoring of a building structure to accommodate various types of control devices and on-line damage detection. The concept of the time-domain approach for integrated vibration control and health monitoring is first introduced. A parameter identification scheme is then developed to identify structural stiffness parameters and update the structural analytical model. Based on the updated analytical model, vibration control of the building using semi-active friction dampers against earthquake excitation is carried out. By assuming that the building suffers certain damage after extreme event or long service and by using the previously identified original structural parameters, a damage detection scheme is finally proposed and used for damage detection. The feasibility of the proposed approach is demonstrated through detailed numerical examples and extensive parameter studies.

Keywords: parameter identification; vibration control; damage detection; integrated system; feasibility study.

1. Introduction

Vibration control and health monitoring of civil engineering structures under harsh environment have been actively investigated in recent years. Several vibration control technologies have been developed for civil engineering structures to mitigate their excessive vibration induced by strong winds, severe earthquakes or other disturbances (Housner *et al*. 1997, Spencer and Nagarajaiah 2003, Kori and Jangid 2008). Several health monitoring systems have also been developed for civil engineering structures to identify their dynamic characteristics and to detect their possible damage after extreme event or long-term service (Aktan *et al*. 2000, Wong *et al*. 2000). Health monitoring systems have been developed and implemented for civil engineering structures to identify their dynamic characteristics and parameters and to detect their possible damage after extreme event or long-term service. Although both vibration control system and health monitoring system need sensors, data acquisition and transmission for real-life implementation, in most of the investigations vibration control and health monitoring have been treated separately according to the primary objective pursued. This separate approach is not practical nor cost-

*Corresponding Author, Associate Professor, E-mail: cbsteven@163.com

effective if civil engineering structures do require both vibration control system and health monitoring system.

Ray and Tian (1999) proposed a method of enhancing modal sensitivity to local damage using feedback control to aid in damage detection. Gattulli and Romeo (2000) proposed the use of an integrated procedure for robust control of oscillations and damage detection of linear structural systems. Sun and Tong (2003) presented a closed-loop control-based damage detection scheme aiming at detecting small damage in controlled structures. These studies, however, focus on actively controlled mechanical systems or small structures and their application to civil structures might be difficult. To this end, Xu and Chen (2008) and Chen and Xu (2008) proposed an integrated vibration control and health monitoring system based on semi-active friction dampers to fulfill model updating, seismic response control and damage detection of building structures. The semi-active friction dampers are used not only to control building vibration but also to provide two states of building stiffness for model updating and damage detection: the original building without any additional stiffness (clamping force is set at zero), and the original building with additional stiffness (damper is in a sticking state). The detailed information can be found in Xu and Chen (2008).

Nevertheless, this integrated control and health monitoring system cannot be applied to the building structures with other types of control devices such as viscous dampers, MR dampers and others. Furthermore, this integrated system conducts model updating and damage detection based on the natural frequencies and mode shapes of the original and damaged structures identified by vibration-based methods. Therefore, this approach is not on line, and the occurrence time of damage events cannot be detected.

This paper presents a general approach in the time domain for integrating vibration control and health monitoring of a building structure to accommodate various types of control devices and on-line damage detection. The concept of the time-domain approach for integrated vibration control and health monitoring is first introduced. A parameter identification scheme is then developed to identify structural stiffness parameters and update the structural analytical model. Based on the updated analytical model, vibration control of the building using semi-active friction dampers against earthquake excitation is carried out. By assuming that the building suffers certain damage after extreme event or long service and by using the previously identified original structural parameters, a damage detection scheme is finally proposed and used for damage detection. The feasibility of the proposed approach is demonstrated through detailed numerical examples and extensive parameter studies.

2. Concept of integrated vibration control and health monitoring

Let us consider a multi-storey shear building subject to earthquake excitation, as shown in Fig. 1. To reduce possible excessive vibration induced by earthquakes, passive or semi-active dampers can be positioned in diagonal braces into the building storey to enhance its vibration energy dissipation capacity. If a semi-active control system is used, the sensory system and the data acquisition and transmission system should be designed properly to provide essential feedback information to determine optimal control signals. The control signals are then sent to the control devices to achieve optimal control forces by which the maximum building response reduction can be achieved.

To identify dynamic characteristics and parameters and to detect possible damage of the building after extreme events or long-term service, the sensory system and the data acquisition and transmission system should be designed as well to provide correct and essential information for parameter identification and damage detection in terms of proper algorithms. Obviously, the semi-active control and health monitoring

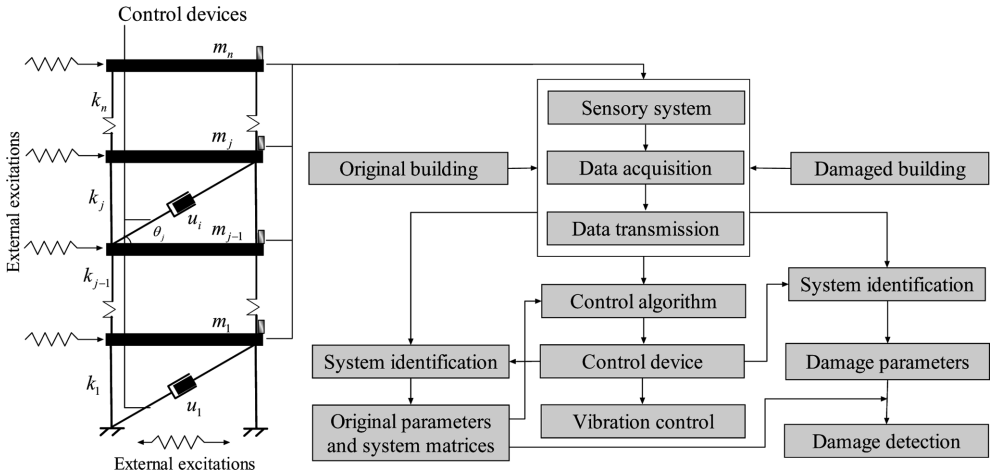

Fig. 1 Integrated vibration control and health monitoring system

both need a sensory system, a data acquisition system and a transmission system. It is desirable to have the common sensory system and the common data acquisition and transmission system for both vibration control and health monitoring of a building structure. This is the basis for the proposed approach to be discussed in this paper.

In the proposed time domain approach, the control forces from the control devices together with the structural responses should be measurable on line. The control forces can therefore be regarded as a series of known external forces. Together with known actual external excitation, the time-domain identification method of a building structure without control devices can then be applied to the building structure with control devices. In such a way, the control devices incorporated into the building should not necessarily be limited to semi-active friction dampers and the model updating and damage detection could be implemented on line. To realize this approach, the first step is to develop a proper time-domain parameter identification method so that the stiffness parameters of a building can be effectively and accurately identified. The original structural model can be updated based on the identified stiffness parameters. Furthermore, the updated structural parameters and building model will facilitate the implementation of structural vibration control and provide the reference for the subsequent vibration control and damage detection. The second step is to present a proper time-domain control algorithm for the updated building model subjected to earthquake excitation. The building may suffer damages after extreme event or long-term service. The last step is to apply the proposed time-domain parameter identification method to the damaged building to identify its structural parameters based on the dynamic responses of both the structure and control devices. By comparing with the structural stiffness parameters before and after damage, the location, severity and time instant of the damage event can be determined consequently. Fig. 1 shows a schematic diagram for the proposed integrated vibration control and health monitoring of a shear building. The details of each step will be introduced in the subsequent sections.

3. Parameter identification of original building

The parameter identification methods in the time domain have been studied in recent years and a number of approaches have been proposed, which include the least-squares method (Wang and Haldar

1994), the maximum likelihood method (Shinozuka *et al*. 1982), the Kalman filter techniques (Hac and Spanos 1990, Loh *et al*. 2000), the substructure approach (Koh *et al*. 1991), and the hybrid identification method (Zhao *et al*. 2006). These identification approaches are developed for the structures without control devices. The parameter identification of controlled structures has not been effectively investigated. The objective of parameter identification in the time domain proposed in this study for controlled structures is to determine the structural parameters based on the measured dynamic responses, external excitations and control forces. The equation of motion for a building structure with control devices under external excitations can be written as

$$\mathbf{M}\ddot{\mathbf{x}}(t) + \mathbf{C}\dot{\mathbf{x}}(t) + \mathbf{K}\mathbf{x}(t) = \mathbf{R}(t) + \mathbf{H}^c\mathbf{u}(t) \tag{1}$$

where **M**, **C** and **K** are the mass, damping and stiffness matrices of the structure respectively, $\mathbf{x}(t)$, $\dot{\mathbf{x}}(t)$ and $\ddot{\mathbf{x}}(t)$ are the displacement, velocity and acceleration responses respectively, $\mathbf{R}(t)$ is the external excitations, $\mathbf{u}(t)$ is the control forces provided by the control devices, and $\mathbf{H}^c$ is the influence matrix reflecting the location of control forces. The Rayleigh damping assumption is adopted to construct the structural damping matrix (Clough and Penzien 2003).

$$\mathbf{C} = \alpha\mathbf{M} + \beta\mathbf{K} \tag{2}$$

where α is the mass damping coefficient; and β is the stiffness damping coefficient. Substituting Eq. (2) into Eq. (1) yields

$$\mathbf{M}\ddot{\mathbf{x}}(t) + \alpha\mathbf{M}\dot{\mathbf{x}}(t) + \beta\mathbf{K}\dot{\mathbf{x}}(t) + \mathbf{K}\mathbf{x}(t) = \mathbf{R}(t) + \mathbf{H}^c\mathbf{u}(t) \tag{3}$$

Eq. (3) can be rewritten as

$$\mathbf{f}_I(t) + \mathbf{f}_{DM}(t) + \mathbf{f}_E(t) = \mathbf{R}(t) + \mathbf{H}^c\mathbf{u}(t) \tag{4}$$

where

$$\mathbf{f}_I(t) = \mathbf{M}\ddot{\mathbf{x}}(t) \tag{5}$$

$$\mathbf{f}_{DM}(t) = \alpha\mathbf{M}\dot{\mathbf{x}}(t) \tag{6}$$

$$\mathbf{f}_E(t) = \mathbf{K}(\beta\dot{\mathbf{x}}(t) + \mathbf{x}(t)) \tag{7}$$

For the shear building investigated in this study, the horizontal stiffness coefficient of the building storey can be selected as the stiffness parameter. The horizontal stiffness coefficient vector θ can be extracted from the elastic restoring force vector $\mathbf{f}_E(t)$ based on the sensitivity analysis as long as the elastic restoring force vector is a linear function of θ (Zhao *et al*. 2006).

$$\mathbf{f}_E(t) = \frac{\partial\mathbf{f}_E(t)}{\partial\gamma^{(1)}}\gamma^{(1)} + \frac{\partial\mathbf{f}_E(t)}{\partial\gamma^{(2)}}\gamma^{(2)} + \ldots\frac{\partial\mathbf{f}_E(t)}{\partial\gamma^{(ne)}}\gamma^{(ne)} \tag{8}$$

$$\mathbf{f}_E(t) = \mathbf{H}(t)\theta \tag{9}$$

where

$$\mathbf{H}(t) = \left[\frac{\partial\mathbf{f}_E(t)}{\partial\gamma^{(1)}}, \frac{\partial\mathbf{f}_E(t)}{\partial\gamma^{(2)}}, \ldots, \frac{\partial\mathbf{f}_E(t)}{\partial\gamma^{(ne)}}\right] \tag{10}$$

$$\theta = (\gamma^{(1)}, \gamma^{(2)}, \ldots, \gamma^{(ne)})^T \tag{11}$$

in which $\gamma^{(i)}$ is the ith horizontal stiffness coefficient, *ne* is the number of building stories. Eq. (4) can then be rewritten as

$$\mathbf{H}(t)\theta = \mathbf{z}(t) \tag{12}$$

where

$$\mathbf{z}(t) = \mathbf{R}(t) + \mathbf{H}^c\mathbf{u}(t) - \mathbf{f}_I(t) - \mathbf{f}_{DM}(t) \tag{13}$$

Eq. (12) can be regarded as the identification equation for the stiffness coefficient vector in the time domain. The coefficient matrix $\mathbf{H}(t)$ can be determined by the sensitivity matrix of $\mathbf{f}_E(t)$ to the stiffness coefficient vector θ and the measured structural responses, which will be shown subsequently. The vector $\mathbf{z}(t)$ can be determined based on the measured external excitations $\mathbf{R}(t)$, the measured control forces $\mathbf{u}(t)$, and the measured structural responses which can be used to further determine $\mathbf{f}_I(t)$ and $\mathbf{f}_{DM}(t)$.

The derivative of $\mathbf{f}_E(t)$ to the stiffness coefficient $\gamma^{(m)}$ of the *m*th storey is

$$\frac{\partial \mathbf{f}_E(t)}{\partial \gamma^{(m)}} = \frac{\partial \mathbf{K}}{\partial \gamma^{(m)}}(\beta\dot{\mathbf{x}}(t) + \mathbf{x}(t)) \tag{14}$$

The sensitivity matrix of the global stiffness matrix $\mathbf{K}$ to the stiffness coefficient of the *m*th storey can be written as

$$\mathbf{S}_{\mathbf{K}}^{(m)} = \frac{\partial \mathbf{K}}{\partial \gamma^{(m)}} = \frac{\partial \mathbf{K}^{(m)}}{\partial \gamma^{(m)}} = [\mathbf{T}^{(m)}]^T \frac{\partial \mathbf{K}_e^{(m)}}{\partial \gamma^{(m)}} \mathbf{T}^{(m)} = [\mathbf{T}^{(m)}]^T \mathbf{S}_{\mathbf{K},e}^{(m)} \mathbf{T}^{(m)} \tag{15}$$

where $\mathbf{K}_e^{(m)}$ is the element stiffness matrix of the *m*th storey in the local coordinate system, $\mathbf{K}^{(m)}$ is the contribution matrix of the element stiffness matrix of the *m*th storey $\mathbf{K}_e^{(m)}$ to the global stiffness matrix $\mathbf{K}$, $\mathbf{S}_{\mathbf{K}}^{(m)}$ is the sensitivity matrix of the global stiffness matrix $\mathbf{K}$ to the *m*th stiffness coefficient $\gamma^{(m)}$, $\mathbf{S}_{\mathbf{K},e}^{(m)}$ is the sensitivity matrix of the element stiffness matrix $\mathbf{K}_e^{(m)}$ to the *m*th stiffness coefficient $\gamma^{(m)}$, $\mathbf{T}^{(m)}$ is the transform matrix from the local coordinate system to the global coordinate system, which is the products of coordinate transformation matrix $\mathbf{T}_a^{(m)}$ and position matrix $\mathbf{T}_c^{(m)}$ of the *m*th storey

$$\mathbf{T}^{(m)} = \mathbf{T}_a^{(m)}\mathbf{T}_c^{(m)} \tag{16}$$

Therefore, the derivative of $\mathbf{f}_E(t)$ with respect to the stiffness coefficient $\gamma^{(m)}$ of the *m*th storey $\frac{\partial \mathbf{f}_E(t)}{\partial \gamma^{(m)}}$ can be written as

$$\mathbf{S}_{\mathbf{f}_E}^{(m)}(t) = \frac{\partial \mathbf{f}_E(t)}{\gamma^{(m)}} = \mathbf{S}_{\mathbf{K}}^{(m)}(\beta\dot{\mathbf{x}}(t) + \mathbf{x}(t)) \tag{17}$$

Eq. (10) can be expressed as

$$\mathbf{H}(t) = [\mathbf{S}_{\mathbf{f}_E}^{(1)}(t), \mathbf{S}_{\mathbf{f}_E}^{(2)}(t), \ldots, \mathbf{S}_{\mathbf{f}_E}^{(ne)}(t)] \tag{18}$$

Eq. (12), the identification equation, can be applied to any sampling instant *t* in theory. However, the zero amplitude and measurement noise in structural response, excitation force, and control force will

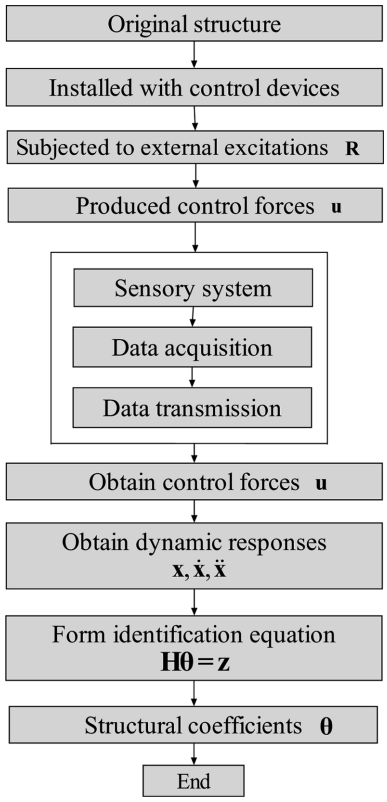

Fig. 2 Flow chart of parameter identification process

affect the quality of identified stiffness coefficients. In this regard, the identification equations at properly-selected sampling instants can be assembled to form an over-determined identification equation for the stiffness coefficient vector

$$\mathbf{H}\boldsymbol{\theta} = \mathbf{z} \tag{19}$$

The flow chart of identification process for stiffness coefficient vector can be seen in Fig. 2.

4. Vibration control of original building

4.1 Modeling of building with control devices

In this section, the semi-active friction dampers are utilized as the control devices positioned in diagonal braces for the building structure for seismic mitigation (see Fig. 1). The corresponding control system shall share the sensory system, data acquisition system and data transmission system with the health monitoring system. The semi-active friction damper is modeled with the components of a linear spring (brace stiffness) and a variable friction damper connected in series, as shown in Fig. 3. The behavior of friction damper is assumed to follow the Coulomb friction model, and the friction force of the damper is therefore linearly proportional to the clamping force when the dynamic friction coefficient μ is considered

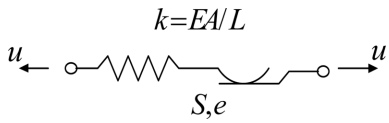

Fig. 3 Mechanical model of semi-active friction dampers

constant and independent on the sliding velocity and the displacement (Ng and Xu 2007, Xu and Ng 2008). The semi-active control force $u(t)$ depends on either the sticking or the slipping state of the damper and it can be written as

$$u(t) = \begin{cases} f^k(t) \text{ if } |f^k(t)| < |f^d(t)| \text{ (sticking)} \\ f^d(t) \text{ if } |f^k(t)| \geq |f^d(t)| \text{ (slipping)} \end{cases} \tag{20}$$

$$f^k(t) = k^d[d(t) - e(t)] \tag{21}$$

in which k^d is the spring stiffness (brace stiffness) of the semi-active friction damper, $f^d(t)$ is the friction force of semi-active friction damper, $f^k(t)$ is the axial force in the semi-active friction damper, $d(t)$ denotes the axial displacement between the two ends of the friction damper, and $e(t)$ is the slip deformation of the friction damper that is given by

$$e(t) = \bar{e}(t) + \left| |d(t) - \bar{e}(t)| - \frac{|u(t)|}{k^d} \right| \operatorname{sgn}(\dot{d}(t)) \tag{22}$$

where $\bar{e}(t)$ is the previously cumulated slip deformation of the friction damper and $\dot{d}(t)$ is the relative velocity between the two ends of the friction damper. The friction force of the semi-active friction damper is given by

$$f^d(t) = \mu N^d(t) \operatorname{sgn}(\dot{d}(t)) \tag{23}$$

where $N^d(t)$ is the clamping force of semi-active friction damper which is time-dependent and determined by the feedback controller. The semi-active control force $u(t)$ is exactly the same as the semi-active friction force $f^d(t)$ if the friction damper slips continuously without sticking. It is noted that if $|f^k(t)|<|f^d(t)|$, the friction damper is in sticking status. The friction damper cannot slip and produce friction control force. Under this circumstance, the friction damper behaves like a pure brace. The force produced by friction damper $f^k(t)$ can be directly calculated as the products of axial deformation and axial stiffness of the friction damper in line with Hooker's Law.

The equation of motion of the building with semi-active friction dampers subjected to seismic excitations can be written as

$$\mathbf{M}\ddot{\mathbf{x}} + \mathbf{C}\dot{\mathbf{x}} + \mathbf{K}\mathbf{x} = -\mathbf{M}\mathbf{I}_g\ddot{x}_g + \mathbf{H}^c\mathbf{u} \tag{24}$$

where $\mathbf{M}$ and $\mathbf{C}$ are the mass and damping matrices of the building respectively, $\mathbf{K}$ is the updated stiffness matrix of the building, $\mathbf{x}$, $\dot{\mathbf{x}}$ and $\ddot{\mathbf{x}}$ are the relative displacement, velocity and acceleration vectors, respectively, with respect to the ground motion, $\ddot{x}_g$ is the ground acceleration, $\mathbf{u}$ is the semi-active control force vector, $\mathbf{I}_g$ is the influence vector for ground acceleration, and $\mathbf{H}^c$ is the influence

matrix reflecting the location of the semi-active friction dampers.

4.2 Global feedback control strategy

The linear quadratic Gaussian (LQG) controller with a modified clipped strategy is applied to the building with semi-active friction dampers. The equation of motion of the building with semi-active friction dampers, that is Eq. (24), is rewritten in state-space form as

$$\dot{\mathbf{z}} = \mathbf{A}\mathbf{z} + \mathbf{B}\mathbf{u} + \mathbf{E}\ddot{x}_g \tag{25}$$

The measured responses $\mathbf{y_m}$ are selected as the absolute acceleration responses of the building floors

$$\mathbf{y_m} = \mathbf{C_m}\mathbf{z} + \mathbf{D_m}\mathbf{u} + \mathbf{F_m}\ddot{x}_g + \mathbf{v} \tag{26}$$

where

$$\mathbf{A} = \begin{bmatrix} 0 & \mathbf{I} \\ -\mathbf{M}^{-1}\mathbf{K} & -\mathbf{M}^{-1}\mathbf{C} \end{bmatrix};\ \mathbf{B} = \begin{bmatrix} 0 \\ \mathbf{M}^{-1}\mathbf{H}^c \end{bmatrix};\ \mathbf{E} = \begin{bmatrix} 0 \\ -1 \end{bmatrix}; \tag{27}$$

in which $\mathbf{z} = [\mathbf{x}\ \dot{\mathbf{x}}]^T$ is the state vector of controlled building, $\mathbf{v}$ is the measurement noise vector, $\mathbf{I}$ is the unit diagonal matrix, $\mathbf{C_m}$, $\mathbf{D_m}$ and $\mathbf{F_m}$ are the reduced-order coefficient matrices of $\mathbf{A}$, $\mathbf{B}$ and $\mathbf{E}$, respectively. The regulated response is expressed as

$$\mathbf{y_{ed}} = \mathbf{C_{ed}}\mathbf{z} + \mathbf{D_{ed}}\mathbf{u} + \mathbf{F_{ed}}\ddot{x}_g \tag{28}$$

where $\mathbf{y_{ed}}$ is the regulated response vector; $\mathbf{C_{ed}}$, $\mathbf{D_{ed}}$ and $\mathbf{F_{ed}}$ are the reduced-order coefficient matrices of $\mathbf{A}$, $\mathbf{B}$ and $\mathbf{E}$, respectively. The acceleration feedback LQG controller is basically designed to minimize a quadratic objective function by weighting the absolute acceleration responses of the building and the control forces, given by

$$J = \lim_{\tau \to \infty} \frac{1}{\tau} E\left[\int_0^{\tau} \{(\mathbf{C_{ed}}\mathbf{z} + \mathbf{D_{ed}}\mathbf{u})^T \mathbf{Q} (\mathbf{C_{ed}}\mathbf{z} + \mathbf{D_{ed}}\mathbf{u}) + \mathbf{u}^T \mathbf{R}\mathbf{u}\} dt\right] \tag{29}$$

where $\mathbf{Q}$ and $\mathbf{R}$ are the weighting matrices for acceleration responses and semi-active control forces, respectively. Based on the separation principle that allows feedback gain and Kalman gain determined separately (Stengel 1986, Skelton 1988), the optimal control force vector is obtained as

$$\mathbf{u} = -\underset{\sim}{\mathbf{K}}\,\widehat{\mathbf{z}} \tag{30}$$

where $\underset{\sim}{\mathbf{K}}$ is the state feedback gain matrix, $\widehat{\mathbf{z}}$ is the estimated state vector described by the steady-state Kalman filter optimal estimator (Stengel 1986, Skelton 1988).

In reality, the control force of a semi-active friction damper depends on its motion status: when the damper is in sticking stage, the control force is equal to the axial force in the brace; and when the damper is in slipping stage, the magnitude of the control force depends on the controllable clamping force and its direction depends on the velocity of the damper (Ng and Xu 2007, Xu and Ng 2008). The closed-loop feedback force determined by Eq. (30) cannot always be achieved by the semi-active friction dampers

because a semi-active friction damper is actually a passive damper with actively-adjustable parameters. Therefore, the following modified clipped control strategy is presented for the friction-based semi-active devices

$$N^d(t) = \begin{cases} u^{LQG}(t)/\mu & \dot{d}(t)\cdot u^{LQG}(t) < 0 \text{ and } \left|u^{LQG}(t)\right| < \mu N^d_{\max} \\ N^d_{\max}\operatorname{sgn}(u^{LQG}(t)) & \dot{d}(t)\cdot u^{LQG}(t) < 0 \text{ and } \left|u^{LQG}(t)\right| \geq \mu N^d_{\max} \\ 0 & \dot{d}(t)\cdot u^{LQG}(t) \geq 0 \end{cases} \tag{31}$$

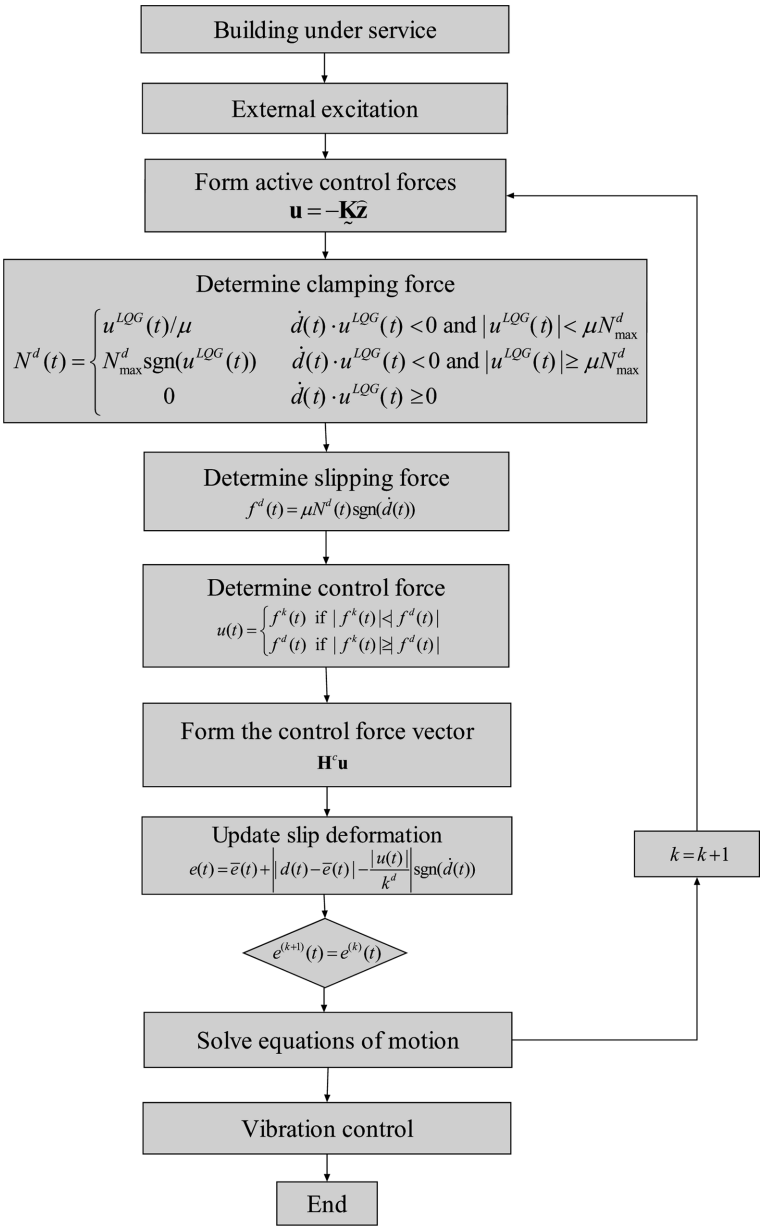

Fig. 4 Flow chart of vibration control process

where u_t^{LQG} is the optimal active control force determined by the LQG controller, $N_{\max}^d$ is the maximum clamping force which can be provided by the semi-active friction damper.

To implement the semi-active control strategy expressed by Eq. (31), the direction of $\dot{d}(t)$ should be determined. Eq. (23) indicates that the control force of the semi-active friction damper $f^d(t)$ has the same direction as $\dot{d}(t)$. The measurement of control forces of damper is thus necessary for determining the direction of $\dot{d}(t)$. As a result, the force transducer incorporated with the semi-active friction damper to measure the control force can be used for not only parameter identification but also vibration control. The flow chart of vibration control process is plotted in Fig. 4.

5. Damage detection

Despite having installed control devices to the building structure, the structure may still suffer some damage after extreme events or long-term service. In this section, the identification scheme introduced in Section 3 is applied to the damaged building for the identification of the reduced stiffness coefficients. By comparing the stiffness coefficients of the undamaged and damaged buildings, the location and severity of the damage events can be determined. For simplicity, the mass and damping matrices of the damaged building are assumed the same as those of the undamaged structure. Similar to the undamaged structure, the identification equation of stiffness coefficients at any time instant can be written as

$$\mathbf{H}^d(t)\theta^d = \mathbf{z}^d(t) \tag{32}$$

where

$$\mathbf{H}^d(t) = [\mathbf{s}_{\mathbf{f}_E}^{d(1)}(t), \mathbf{s}_{\mathbf{f}_E}^{d(2)}(t), \ldots, \mathbf{s}_{\mathbf{f}_E}^{d(ne)}(t)] \tag{33}$$

$$\theta^d = (\gamma^{d(1)}, \gamma^{d(2)}, \ldots, \gamma^{d(ne)})^T \tag{34}$$

$$\mathbf{z}^d(t) = \mathbf{R}(t) + \mathbf{H}^c\mathbf{u}^d(t) - \mathbf{f}_I^d(t) - \mathbf{f}_{DM}^d(t) \tag{35}$$

$$\mathbf{f}_I^d(t) = \mathbf{M}\ddot{\mathbf{x}}^d(t) \tag{36}$$

$$\mathbf{f}_{DM}^d(t) = \alpha\mathbf{M}\dot{\mathbf{x}}^d(t) \tag{37}$$

$$\mathbf{f}_E^d(t) = \mathbf{K}^d(\beta\dot{\mathbf{x}}^d(t) + \mathbf{x}^d(t)) \tag{38}$$

$$\mathbf{s}_{\mathbf{f}_E}^{d(m)}(t) = \frac{\partial\mathbf{f}_E^d(t)}{\gamma^{d(m)}} = \mathbf{S}_{\mathbf{K}}^{(m)}(\beta\dot{\mathbf{x}}^d(t) + \mathbf{x}^d(t)) \tag{39}$$

in which $\gamma^{d(m)}$ is the mth stiffness coefficient of the damaged building; and the superscript d represents the damaged case. Assembling the identification equation (Eq. (32)) at properly-selected sampling instants would result in the over-determined identification equation for the stiffness coefficients of the damaged building, as discussed by Zhao *et al*. (2006).

$$\mathbf{H}^d\theta^d = \mathbf{z}^d \tag{40}$$

Once the stiffness coefficients of the damaged building are found, the damage location and severity can

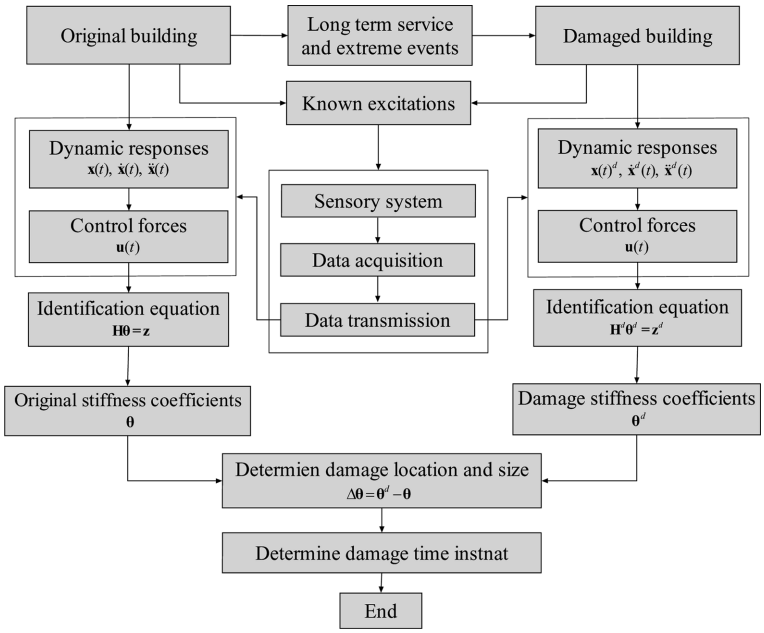

Fig. 5 Flow chart of damage detection process

be determined by the following equation

$$\Delta\theta = \theta^d - \theta \tag{41}$$

By applying the above equation to the time histories recorded by the structural health monitoring system continuously, the occurrence time of damage event can be determined almost on line. The flow chart of damage detection process is plotted in Fig. 5.

6. Numerical investigation

6.1 Description of an example building

The five-storey shear building demonstrated in Fig. 6 is selected as an example building to examine the feasibility of the proposed time-domain approach for integrated vibration control and health monitoring. The example building has the same storey height of 3 m. The mass and the horizontal storey (shear) stiffness of the original building without damage are uniform for all storeys with mass $m = 5.1\times10^3$ kg and stiffness $k = 1.334\times10^7$ N/m. The equation of motion of the building is solved using the Newmark-β method with a time step of 0.002s. The two factors in the Newmark-β method are selected as 1/2 and 1/4, respectively. The Rayleigh damping assumption is adopted to construct the structural damping matrix. The damping ratios in the first two modes of vibration of the building are assumed to be 0.02. A semi-active friction damper with a diagonal brace is used to connect two neighboring floors. The same arrangement is made for each storey of the building with the same damper as shown in Fig. 6. The stiffness ratio (SR) of the brace stiffness to the horizontal stiffness of the building storey is defined as

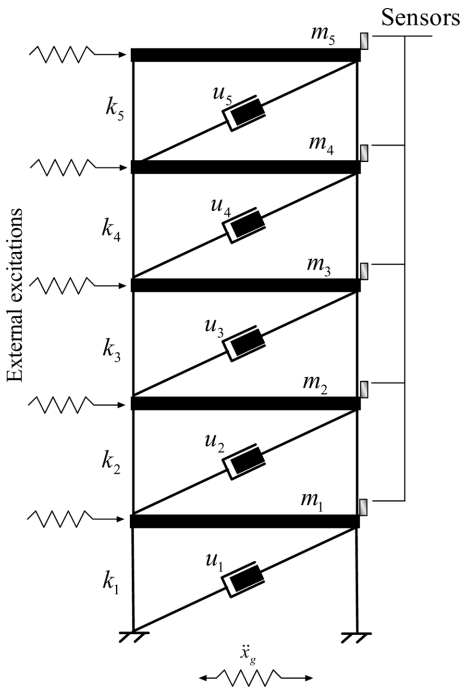

Fig. 6 Five storey shear building with semi-active friction dampers

$$SR = \frac{K_d}{K_s} \tag{42}$$

where K_s is the horizontal stiffness coefficient of the building storey, and K_d is the stiffness coefficient of the brace.

6.2 Parameter identification of the example building

6.2.1 Parameter identification without noise contamination

For the purpose of parameter identification, an external dynamic force P1 is applied to the first floor to excite the building (see Fig. 7). The dynamic force is assumed to be a white noise random process with a peak value of 5.4 kN, and the time history of the force is simulated by the computer with a sampling frequency of 500 Hz. The clamping force of the semi-active friction damper is set as 5 kN. The displacement, velocity and acceleration responses of all the floors and the control forces of all the semi-active friction

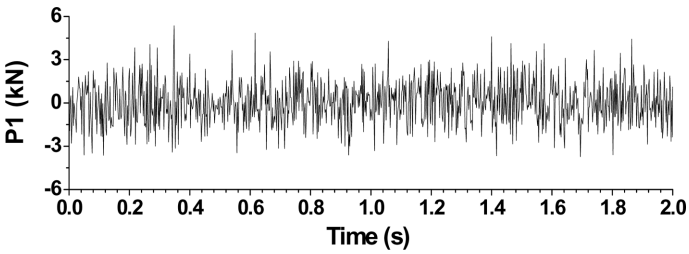

Fig. 7 Time history of external dynamic force P1

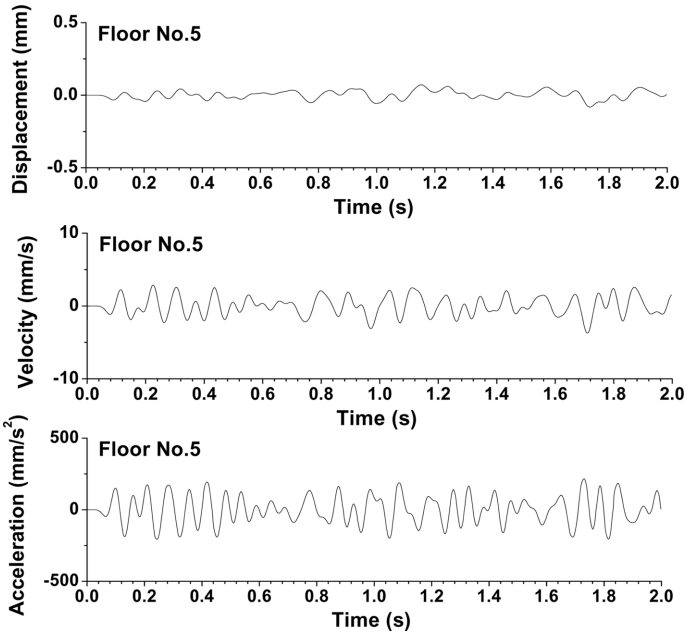

Fig. 8 Time histories of dynamic responses at the top floor

dampers are computed and taken as the measured results. For the five-storey shear building concerned, the horizontal storey stiffness coefficient vector to be identified can be expressed by

$$\theta = [k_1, k_2, k_3, k_4, k_5]^T \tag{43}$$

The time histories of displacement, velocity, and acceleration responses of the building at the top floor are shown in Fig. 8. Fig. 9 demonstrates the time histories of control forces for all the five semi-active friction dampers. By using the measured dynamic responses, control forces and external excitation and considering no noise contamination, the stiffness coefficients of the building can be identified, and the identified results are shown in Fig. 10. It can be seen that the actual values of horizontal stiffness coefficients can be identified exactly for all the five storeys when the noise contamination is not considered.

For the semi-active friction dampers used in this study for integrated vibration control and health monitoring, the clamping forces of the semi-active friction dampers can be set as zero to create the status of the building without any control forces. The stiffness coefficients of the building in such a case are also identified to compare with the building with control devices. The results show that without considering noise contamination, the identified stiffness coefficients from the building with control devices are exactly the same as those from the building without control devices.

6.2.2 Parameter identification with noise contamination

In practice, the noise contamination is unavoidable in the measured dynamic responses, external dynamic forces and control forces. Therefore, the effects of measurement noise on the identification quality of stiffness coefficients should be examined. The measurement noise, which is assumed to be a white noise random process, is simulated and added to the dynamic responses, control forces and external force according to a given noise intensity. The noise intensity is defined as the ratio of the root mean

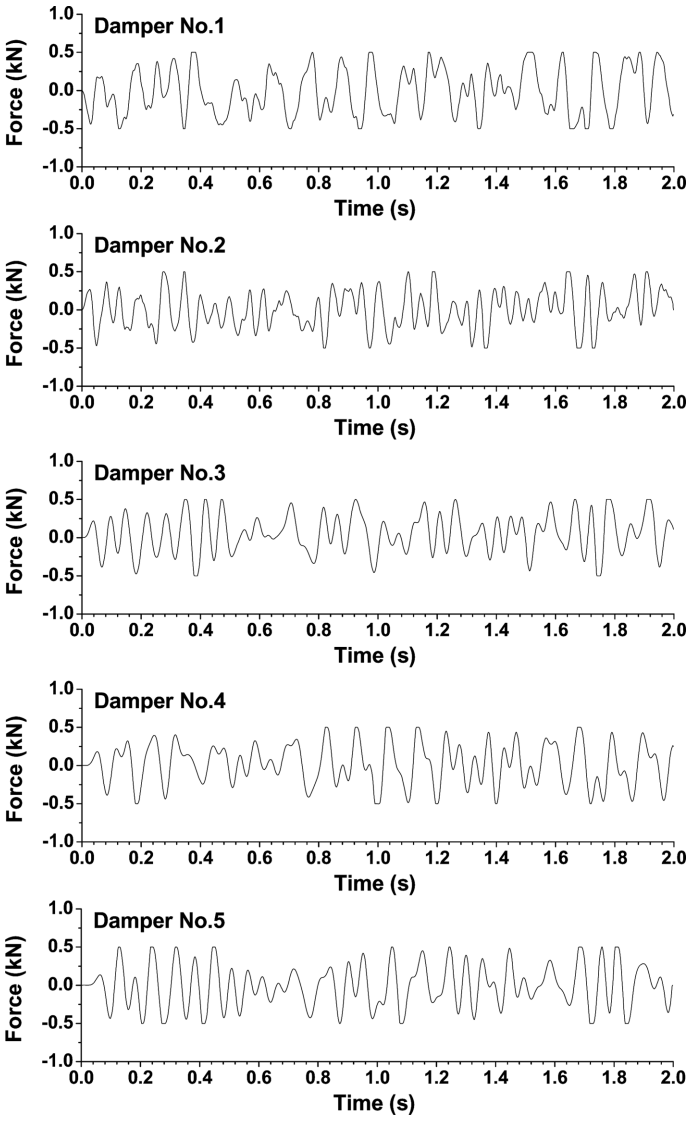

Fig. 9 Time histories of control forces

square (RMS) of the noise to the RMS of the time history of original signal

$$\text{Noise intensity} = \frac{\text{RMS(noise)}}{\text{RMS(signal)}} \times 100\% \tag{44}$$

Because the measurement noise considered in this study is assumed to be normally distributed white noise, the amplitude of measurement noise at one frequency is the same as that at other frequency in the frequency domain. In the time domain, the amplitude of measurement noise at most time instants is below a certain value. For instance, for a normally distributed white noise the noise amplitude at 95% of the sampling points of measurement noise time history is below 1.645 times its RMS. Since the amplitude of structural response at each time instant is different, the relative error induced by measurement noise would

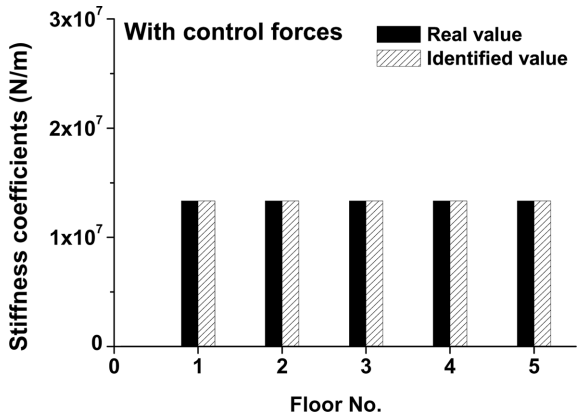

Fig. 10 Identification results of stiffness coefficients without noise contamination

be different from time instant to time instant. According to the noise intensity defined in Eq. (44), the relative noise level will be small for the structural response of large amplitude in general. Furthermore, it is not necessary to take all the time instants (the sampling points) in one time history into full consideration when using the identification equation. Therefore, based on the above observations Zhao *et al.* (2006) proposed an amplitude-selective filtering procedure to filter the structural responses below a preset threshold. Only the structural responses above the given threshold are retained in the identification process so as to reduce the effect of measurement noise and at the same time to improve the identification quality. The criterion used to determine the threshold is the number of the retained sampling points in the structural response time histories. The number of retained sampling points should be smaller compared with the total number of sampling points, but it should be large enough to satisfy the effective solution to the identification equation. For a single-response time history $\mathbf{x}_i$ of dimension n, if the number of retained sampling points is set to m, the retained structural response time history after the filtering can be expressed as

$$\mathbf{x}_j = \{x_i | x_i > x^*\} \tag{45}$$

where x^* is the (n-m) largest value in the original time history $\mathbf{x}_i$. For more than one structural response time history, in consideration that different types of structural responses are involved and the same noise level is assigned to each measured time history, the sampling points are discarded one by one starting from the point with the smallest response until the retained number reaches the given number but this procedure should be applied to all the response time histories with an even chance.

Three noise intensities, 0.5%, 1.0% and 2%, are introduced to the structural dynamic responses, control forces and external dynamic force to assess the effects of noise contamination on the identification quality of the stiffness coefficients. The retained number of sampling points is set at 100 following Eq. (45). It can be seen from Fig. 11(a) that the identification errors gradually increase with the increasing noise intensity. The maximum relative identification error in the stiffness coefficients is about 1.6% for 2% noise intensity. The above identification observations are made based on the white noise excitation acting on the first floor. The identification cases with other kinds of excitations such as sinusoidal excitation acting on other floors of the building are also analyzed. Similar observations can be made to those reported in this section. Plotted in Fig. 11(b) are the relative identification errors in the stiffness coefficients at the three levels of noise for the cases without control forces. It can be seen that identification errors increase with

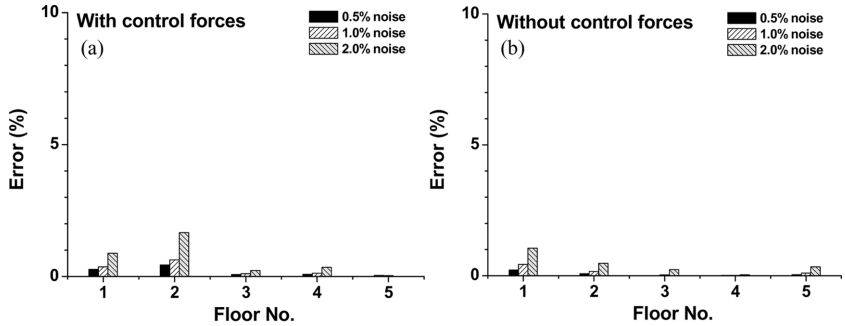

Fig. 11 Identification results of stiffness coefficients with noise contamination: (a) with control force and (b) without control force

the increase in noise intensity. The maximum relative identification error in the stiffness coefficients is about 1% for 2% noise intensity. The identification quality without control forces is slightly better than that with control forces. It is noted that the measured time histories of control forces utilized in the identification are also polluted by the noise contamination.

In vibration control, the stiffness ratio of dampers may affect the control performance. The effects of stiffness ratio on the identification quality are also investigated. The numerical results indicate that the stiffness ratio has no obvious effects on the identification quality. This is because the control forces measured directly by force transducers are used in the identification.

6.3 Seismic response control of the example building

6.3.1 Seismic input and evaluation index

To evaluate the control performance, four seismic records are selected as inputs to the example building: (1) El Centro NS (1940); (2) Hachinohe NS (1968); (3) Northridge NS (1994); and (4) Kobe NS (1995). The original peak ground accelerations of the four seismic records are 3.417, 2.250, 8.2676 and 8.1782 m/s^2, respectively. The original time histories of the four seismic records are scaled to have the same peak ground accelerations of 4.0 m/s^2 to facilitate the comparison. The stiffness matrix of the example building is constructed using the stiffness coefficients identified with control devices and 1% noise level. The stiffness ratios of all the five semi-active friction dampers are assigned the same value of 0.9. Five accelerometers and five force transducers with one accelerometer and one force transducer for one storey are necessary to realize the feedback control. In the numerical investigation of control performance, the corresponding computed building responses and damper forces are taken as the relevant feedback instead of the signals from the sensors in practice. The control performance is evaluated in terms of a vibration reduction factor (VRF) defined as follows (Chen and Xu 2008)

$$VRF = \frac{Z_{nc} - Z_{co}}{Z_{nc}} \tag{46}$$

where Z_{nc} is the maximum response (either displacement, velocity or acceleration) of a given building floor without control; and Z_{co} is the maximum response of the same quantity of the same floor with control.

6.3.2 Evaluation of control performance

In the implementation of the proposed control strategy, the two weighting matrices **Q** and **R** are selected as the unit diagonal matrix multiplied by a factor. The optimum factor is found to be 2.1×10^5 for **Q** and 0.016 for **R**. To determine the maximum clamping force $N_{\max}^{d}$, which can be provided by the semi-active friction damper, the maximum axial force in the brace of the example building without semi-active control is computed with the El Centro NS seismic input. The maximum axial force is then taken as the maximum slipping force.

Figs. 12(a)-(c) depict the variations of the peak displacement, velocity, and acceleration responses of the example building for three cases: (1) original building without control; (2) original building with braces; (3) semi-active control. It can be seen that the installation of common braces can reduce the maximum displacement response of the building but it can increase the maximum acceleration response compared with the original building. The peak responses of displacement, velocity and acceleration of all the building floors under semi-active control are substantially reduced in comparison with those of the original building. The feasibility of the proposed integrated procedure also depends on the brace (damper) stiffness for both vibration control and parameter identification. Fig. 13 shows the variations of VRF of displacement, velocity and acceleration responses of the top floor with respect to SR under semi-active control. It is observed that the vibration reduction factors for all the three responses increase rapidly at the beginning.

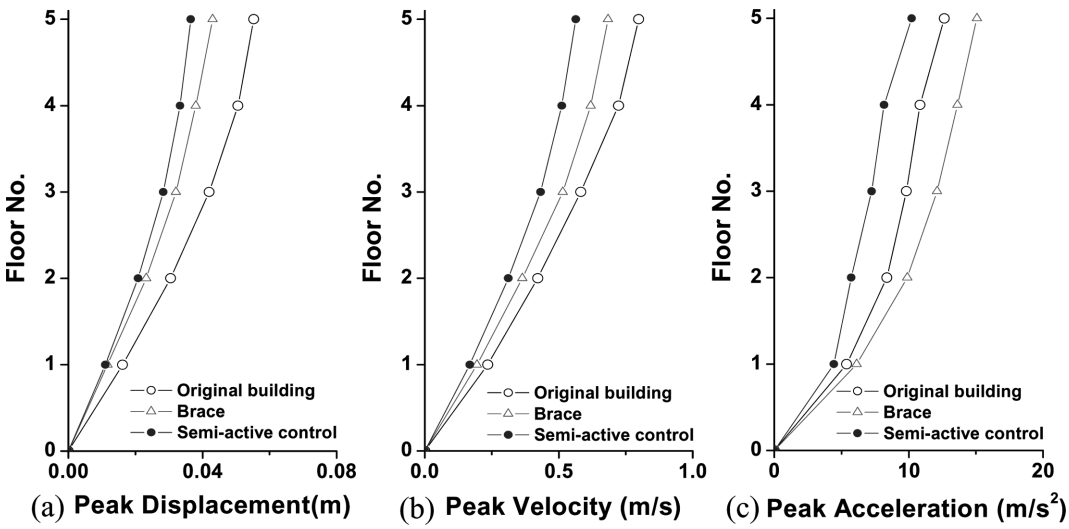

Fig. 12 Comparison of control performance for different cases: (a) displacement, (b) velocity and (c) acceleration

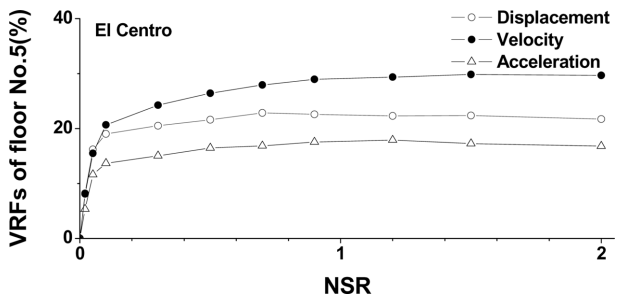

Fig. 13 Variations of VRFs with SR

Afterwards, the vibration reduction factors increase only slightly with increasing stiffness ratio. When it reaches above 0.9, the stiffness ratio has almost no effect on the vibration reduction factors. The similar results are found for other building floors. As a result, the optimum stiffness ratio for seismic response control of the example building can be taken as 0.9.

6.3.3 Control performance under other seismic inputs

The seismic responses of the example building subjected to other three ground motions are also investigated and similar investigations to those under El Centro NS earthquake can be made. Numerical study indicates that the optimum stiffness ratio found from the case of the El Centro earthquake remains almost unchanged for the other three seismic inputs. Two widely-accepted sets of normalized performance indices are adopted, to compare the control performance under different earthquakes. The first set of the performance indices is related to the building responses (Ohtori *et al*. 2004), which include peak- and RMS- based inter-storey drift ratios (J_1 and J_3) and peak- and RMS-based absolute acceleration responses (J_2 and J_4), as expressed by

$$J_1 = \left\{ \frac{\max\limits_{t,i} |dx_i(t)|/h_i}{\delta^{\max}} \right\} \tag{47}$$

$$J_2 = \left\{ \frac{\max\limits_{t,i} |\ddot{x}_{ai}(t)|}{\ddot{x}_a^{\max}} \right\} \tag{48}$$

$$J_3 = \left\{ \frac{\max\limits_{t,i} \|dx_i(t)\| h_i}{\|\delta^{\max}\|} \right\} \tag{49}$$

$$J_4 = \left\{ \frac{\max\limits_{t,i} \|\ddot{x}_{ai}(t)\|}{\|\ddot{x}_a^{\max}\|} \right\} \tag{50}$$

where $dx_i(t)$ is the inter-storey drift of the ith story of the building with control, h_i is the height of the ith story, $dx_i(t)/h_i$ is the inter-storey drift ratio of the ith story of the building with control, $\delta^{\max}$ is the maximum inter-storey drift ratio of the original building without any control, $\ddot{x}_{ai}$ is the absolute acceleration response of the ith floor of the building with control, $\ddot{x}_a^{\max}$ is the maximum absolute acceleration response of the ith floor of the building without any control. The RMS response quantities within the time duration t_f under each earthquake are calculated by

$$\|\cdot\| = \sqrt{\frac{1}{t_f}\int_0^{t_f} [\cdot]^2 dt} \tag{51}$$

The sign $\max\limits_{t,i}$ means to find the maximum value within the given time duration first and among all the building stories/floors afterwards.

The second set of performance indices are related to the capacity of control devices. The peak-based control force (J_5) is

$$J_5 = \left\{ \frac{\max\limits_{t,l} |f_l(t)|}{W} \right\} \tag{52}$$

Table 1 Performance indices for semi-active control

Index	El Centro	Hachinohe	Northridge	Kobe
J_1 (peak drift ratio)	0.6875	0.7042	0.7307	0.5246
J_2 (peak acc.)	0.8086	0.8042	0.7334	0.5775
J_3 (rms drift ratio)	0.4947	0.5449	0.5070	0.4271
J_4 (rms acc.)	0.5301	0.5660	0.5375	0.4428
J_5 (control force)	0.0940	0.0967	0.1363	0.1026

where $f_l(t)$ is the control force generated by the lth control device; and W is the seismic weight of the building, that is, the total weight of all the building floors in this study.

Table 1 shows the performance indices of the controlled building for the four seismic inputs, respectively. It is observed that the developed control approach by using semi-active friction dampers can effectively reduce both the peak and RMS responses of the example under all the four seismic inputs. The control performance on RMS responses (J_1 and J_2) is better in comparison with that of peak responses (J_3 and J_4) for all the four earthquakes. As far as the rms responses are concerned, the performance indices of drift ratio are slightly superior to those of acceleration responses. Similar observations can be made from the peak response except for the case of Northridge earthquake. The control force indices for different cases are very close except for the case of Northridge earthquake.

6.4 Damage detection of the example building

The feasibility of the damage detection scheme in the proposed integrated approach for identifying different damage severities and locations is examined in this section. The effect of noise contamination on the damage detection quality is also assessed. Two damage scenarios are taken into consideration in this section: (1) single damage event with 20%, 30%, 40% and 50% stiffness loss, respectively, at the first storey of the example building; and (2) double damage event with 20% and 30% stiffness loss at the first and fourth storey respectively. The two levels of measurement noise of 1% and 2% are considered in the damage detection. The external excitation and the slipping force of the semi-active friction damper adopted are the same as those used in the stiffness identification. In addition, the damage detection of the structures without control forces is also carried out for comparison. The dynamic responses of all floors to the input dynamic force are computed. The measurement noise is simulated and added to the dynamic responses according to a given noise intensity. The retained sampling points are selected as 100 using the amplitude-selective filtering procedure.

The damage size, which is defined as the absolute value of the difference between the detected stiffness and the original stiffness divided by the original stiffness, is computed for the single damage event in the first storey. The results are indicated in Figs. 14 (a) to (d) for 20%, 30%, 40% and 50% stiffness loss cases, respectively, with control forces. It can be seen that without measurement noise, the proposed detection scheme can accurately determine the damage location and size. With measurement noise involved, the proposed detection scheme can still determine the damage location and size satisfactorily. With the increase of measurement noise intensity, the damage size detected is less accurate. Fig. 15 demonstrates the damage sizes for the double damage events. It is seen that without measurement noise, the proposed detection scheme can exactly determine the damage location and size. With measurement noise considered, the damage location and size can still be effectively determined but the accuracy of damage detection is reduced with the increase of measurement noise intensity. The damage sizes for the single and double

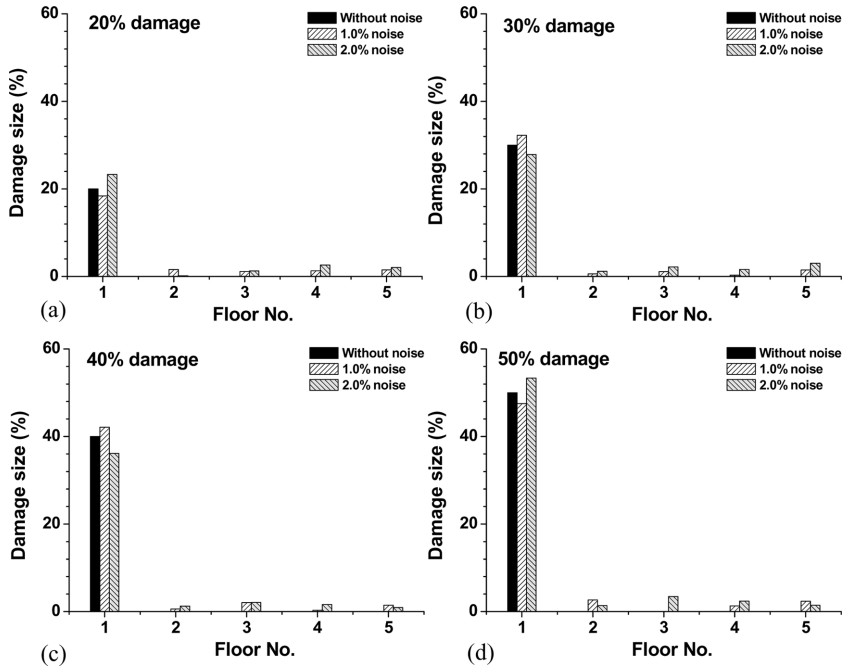

Fig. 14 Damage detection results for single damage event with control forces

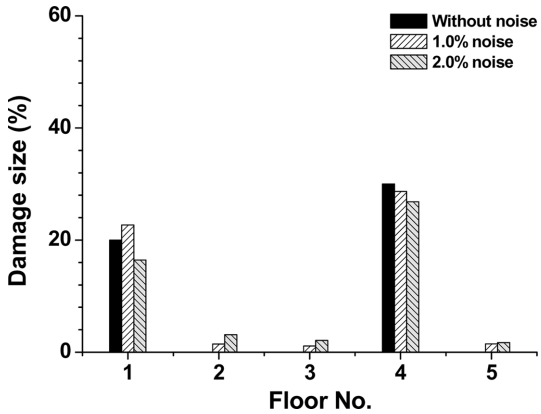

Fig. 15 Damage detection results for double damage events with control forces

damage events without control forces are also computed and the results are shown in Figs. 16 and 17, respectively. Similar conclusions can be reached to those obtained with known control forces. The comparison of the identification quality between the cases with/without control forces demonstrates that the stiffness coefficients can be accurately determined without noise contamination in both cases. With the introduction of noise contamination, the identification quality without control forces is slightly better than those with control forces.

The occurrence time of damage events can also be detected by using the proposed time-domain method. Let us consider a case in which the duration of the external dynamic force is 60 seconds and the stiffness of the first storey is suddenly reduced by 30% at the 20-second time instant. The computed structural responses, control forces and external dynamic forces of 60 seconds are used for the identification. The

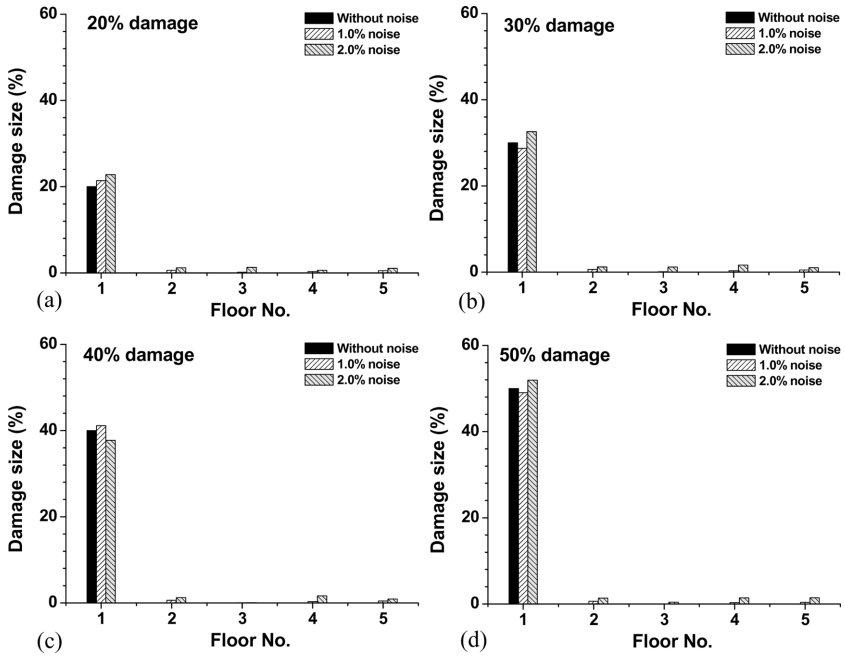

Fig. 16 Damage detection results for single damage event without control forces

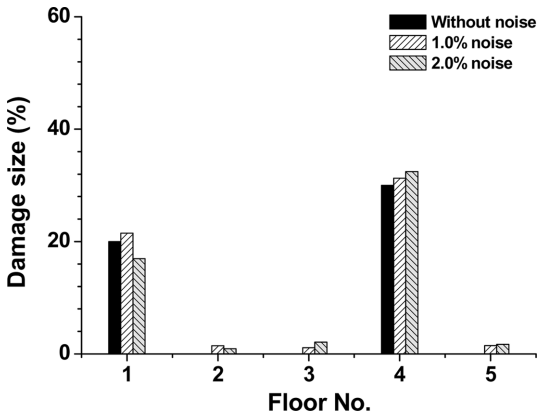

Fig. 17 Damage detection results for double damage event without control forces

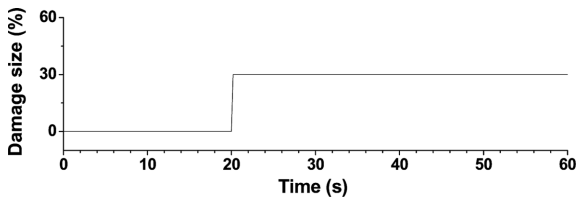

Fig. 18 Detection results for occurrence time of damage event

identified damage size with an interval of 100 sampling points is plotted in Fig. 18 against the time. It is seen that the occurrence time of the damage event can be found at almost the 20-second time instant.

7. Conclusions

A general approach for integrating vibration control and health monitoring of a building structure to accommodate various types of control devices and on-line damage detection has been proposed in this paper. For parameter identification, the identification scheme developed in the time domain has been applied to a five-storey shear building installed with semi-active friction dampers. The numerical results demonstrated that the identification of structural stiffness coefficients first and the updating of stiffness matrix afterwards could be successfully carried out by using the proposed identification scheme. The identification quality for the building with control devices remained almost the same as that for the building without control devices even with small noise contamination.

For vibration control, the semi-active control strategy based on the global feedback control algorithm has been proposed for the semi-active friction dampers to reduce seismic responses of the building. The numerical results demonstrated that by using the building model with updated structural parameters and the optimum stiffness ratio the structural seismic responses could be substantially reduced using the semi-active friction dampers.

For damage detection, the detection scheme by applying the identification scheme to both the original building and damaged building has been proposed. The numerical results demonstrated that the damage size, location and occurrence time could be accurately identified if noise contamination was not considered. The quality of damage detection gradually decreased with the increasing noise intensity. It is worthwhile to point out that although the feasibility of the proposed approach was demonstrated for building structures by using semi-active friction dampers, the proposed approach could actually be applied to building structures with other types of control devices. The integrated health monitoring and vibration control of structures with complicated configuration are not to be carried out in this study. This may deserve further investigation.

Acknowledgements

The writers are grateful for the financial support from the National Natural Science Foundation of China (Grants NNSF-50708083 and 50830203) and The Hong Kong Polytechnic University through an Inter-Faculty Research Grant.

References

Aktan, A.E., Catbas, F.N., Grimmelsman, K.A. and Tsikos, C.J. (2000), "Issues in infrastructure health monitoring for management", *J. Eng. Mech.-ASCE*, **126**(7), 711-724.

Chen, B. and Xu, Y.L. (2008), "Integrated vibration control and health monitoring of building structures using semi-active friction dampers: Part II-numerical investigation", *Eng. Struct.*, **30**(3), 573-587.

Clough, R.W. and Penzien, J. (2003), *Dynamic of structures*, 3rd Edition, McGraw-Hill, New York.

Gattulli, V. and Romeo, F. (2000), "Integrated procedure for identification and control of MDOF structures", *J. Eng. Mech.-ASCE*, **126**(7), 730-737.

Hac, A. and Spanos, P.D. (1990), "Time domain method for parameter system identification", *J. Vib. Acoust.*, **112**(3), 281-287.

Housner, G.W., Bergman, L.A., Caughey, T.K., Chassiakos, A.G., Claus, R.O., Masri, S.F., Skelton, R.E., Soong, T.T., Spencer, B.F. Jr. and Yao, J.T.P. (1997), "Structural control: past present, and future", *J. Eng. Mech.-ASCE*, **123**(9), 897-971.

Koh, C.G., See, L.M. and Balendra, T. (1991), "Estimation of structural parameters in time domain: a substructure approach", *Earthq. Eng. Struct. D.*, **20**(8), 787-801.

Kori, J.G. and Jangid, R.S. (2008), "Semi-active friction dampers for seismic control of structures", *Smart Struct. Syst.*, **4**(4), 493-515.

Loh, C.H., Lin, C.Y. and Huang, C.C. (2000), "Time domain identification of frames under earthquake loadings", *J. Eng. Mech.-ASCE*, **126**(7), 693-703.

Ng, C.L. and Xu, Y.L. (2007), "Semi-active control of a building complex with variable friction dampers," *Eng. Struct.*, **29**(6), 1209-1225.

Ohtori, C.L., Christenson, R.E., Spencer, B.F. Jr. and Dyke, S.J. (2004), "Benchmark control problems for seismically excited nonlinear buildings", *J. Eng. Mech.-ASCE*, **130**(4), 366-385.

Ray, L.R. and Tian, L. (1999), "Damage detection in smart structures through sensitivity enhancing feedback control", *J. Sound Vib.*, **227**(5), 987-1002.

Shinozuka, M., Yun, C.B. and Imai, H. (1982), "Identification of linear structural dynamic system", *J. Eng. Mech. Div., ASCE*, **108**(6), 1371-1390.

Skelton, R.E. (1988), *Dynamic system control: Linear systems analysis and synthesis*, Wiley, New York.

Spencer, B.F. Jr. and Nagarajaiah, S. (2003), "State of the art of structural control", *J. Struct. Eng.-ASCE*, **129**(7), 845-856.

Stengel, R.F. (1986), *Stochastic optimal control: Theory and application*, Wiley, New York.

Sun, D.C. and Tong, L.Y. (2003), "Closed-loop based detection of debonding of piezoelectric actuator patches in controlled beams", *Int. J. Solids Struct.*, **40**(10), 2449-2471.

Wang, D. and Haldar, A. (1994), "Element-level system identification with unknown input", *J. Eng. Mech.-ASCE*, **120**(1), 159-176.

Wong, K.Y., Chan, K.W.Y., Man, K.L., Mak, W.P.N. and Lau, C.K. (2000), "The use of structural health monitoring system in operation and maintenance of cable-supported bridges", *Proceedings of the Structural Symposium 2000-Highway and Railway Structures*, Hong Kong, China.

Xu, Y.L. and Chen, B. (2008), "Integrated vibration control and health monitoring of building structures using semi-active friction dampers: Part I-methodology", *Eng. Struct.*, **30**(7), 1789-1801.

Xu, Y.L. and Ng, C.L. (2008), "Seismic protection of a building complex using variable friction damper: Experimental investigation", *J. Eng. Mech.-ASCE*, **134**(8), 637-649.

Zhao, X., Xu, Y.L., Li, J. and Chen, J. (2006), "Hybrid identification method for multi-story buildings with unknown ground motion: theory", *J. Sound Vib.*, **291**(1-2), 215-239.

CC